Towards reliable micromagnetic detection of white etching layers in deep drilled quenched and tempered steels

S. Strodick*, D. Steffens, F. Walther

Chair of Materials Test Engineering (WPT), TU Dortmund University

* Corresponding author: simon.strodick@tu-dortmund.de

R. Schmidt, A. Zabel, D. Biermann

Institute of Machining Technology (ISF), TU Dortmund University

Abstract

Ultrafine-grained white etching layers (WEL) can be formed in the machining of steels, titanium alloys and nickel-based superalloys due to high forces and temperatures in the contact area of the tool and the workpiece. In general, these layers are associated with very high hardness and brittleness as well as (tensile) residual stresses. These mechanical properties of WEL can have a severely negative impact on the lifetime and reliability of components. As a result, it is of crucial importance to reliably detect WEL, understand the underlying mechanisms and physical relationships in their formation and finally control their emergence in machining. Currently, WEL are usually detected using destructive metallographic analyses. In recent years, therefore, the applicability of alternative non-destructive methods for the reliable detection of WEL has been increasingly investigated. In this context, methods such as X-ray diffraction, acoustic emission (AE) and eddy current testing were used. The analysis of magnetic Barkhausen noise (MBN) was identified as a particularly suitable method for the detection of WEL in steels with a very high potential for application in production technology.

In this study, MBN analysis is employed for the time-efficient and non-destructive detection of WEL in deep drilled components made of the quenched and tempered steel AISI 4140. It is shown that WEL form in drilling, especially at high cutting speeds and feeds. The use of coated guide pads and cutting edges promotes the formation of WEL. Hardness in the WEL exceeds the hardness of the bulk material up to three times. Specimens with thick WEL can be separated from specimens free of WEL by significantly lower maximum magnetic Barkhausen noise amplitudes.

1 Introduction

Quenched and tempered steels exhibit a unique combination of strength and ductility, thus offering excellent toughness. At the same time, they are relatively cheap and widely available in large quantities and in a wide range of shapes. Throughout the past decades, these features have made quenched and tempered steels a key material for numerous applications, especially when it comes to dynamically loaded high-performance components, such as e.g. shafts of powertrain systems, gears or connecting rods. When machining these components e.g. by drilling, milling or turning, their surface integrity (SI) is substantially altered, e.g. with respect to microstructure, residual stresses and micro-hardness. Driven by the complex interrelations between machining, the resulting SI and the performance of components, numerous scientific endeavors have been undertaken in the past decades to thoroughly design machining processes, taking into account not only geometrical accuracy, productivity, etc. but also the resulting SI of machined components [1–3]. One particular form of machining-induced SI modification is the formation of ultrafine-grained and brittle layers, named white etching layers (WEL). A detailed overview of the formation mechanisms of WEL in machining, the properties associated with them and detection methods is given by Brown et al. in [4] and [5]. WEL are usually associated with embrittled surfaces and elevated tensile residual stresses. Due to these mechanical properties, WEL oftentimes promote the initiation and growth of cracks and subsequently reduce the fatigue life of components.

For the machining of bores into quenched and tempered steels with large length-to-diameter ratios (l/d > 10) and large diameters (d ≥ 6 mm), the Boring Trepanning Association (BTA) deep hole drilling process, also called single tube system drilling, is usually employed. Components machined by this process include the landing gears of airplanes, drill collars and hydraulic cylinders. The fundamentals of deep hole drilling as well as a detailed explanation of the process characteristics of BTA deep hole drilling is given by Biermann et al. in [6]. In BTA deep hole drilling chips are removed by the cutting edges of the tool and the machined surfaces are subsequently smoothened and burnished by guide pads. Thus, a tandem of effects on the subsurface zones needs to be considered when analyzing SI resulting from BTA deep hole drilling. In previous investigations, it was shown that WEL tend to form in BTA deep hole drilling when using elevated feed rates and cutting speeds [7,8]. These layers could be detected by means of magnetic Barkhausen noise (MBN) analysis. MBN analysis is a non-destructive technique for assessing various material properties like grain size, hardness and residual stress state by analyzing the response of the material to an external periodically changing magnetic field. The fundamentals of this technique are explained along with some examples of applications of MBN analysis by Baak et al. in [9].

In this study, the effects of tool coating, feed rate and cutting speed in BTA deep hole drilling on the resulting SI of bores are analyzed. Metallographic analyses of longitudinal and transverse sections are carried out as well as microhardness mappings of the subsurface zones. The results serve as references for MBN analyses.

2   Materials and methods

Round bars of quenched and tempered AISI 4140 (42CrMo4+QT, 1.7225) with an outer diameter of $d_{outer} = 75$ mm and a length of $l = 250$ mm were machined by BTA deep hole drilling. Drilling of bores with an inner diameter of $d_{inner} = 60$ mm was performed using a deep hole drilling machine Giana GBB 560 (Fig. 1a). A BTA drill head type 12 by Botek Praezisionsbohrtechnik GmbH was equipped with an inner and an outer cutting insert and guide pads. To investigate the influence of the tool coating on SI, guide pads and cutting edges were used in an uncoated state as well as with a coating of titanium nitride (TiN). The substrate material of the guide pads was cemented carbide of grades K10 (for uncoated guide pads) and P20B (for TiN-coated guide pads). Drilling took place at four cutting speeds ($v_c = 60$; 80; 100; 120 m/min) in combination with three feed rates ($f = 0.150$; 0.225; 0.300 mm). For lubrication and chip removal, the deep drilling oil Berucut RMO TC 22 was supplied with a pressure of $p = 11$ bar and a flow rate of $\dot{V} = 300$ l/min.
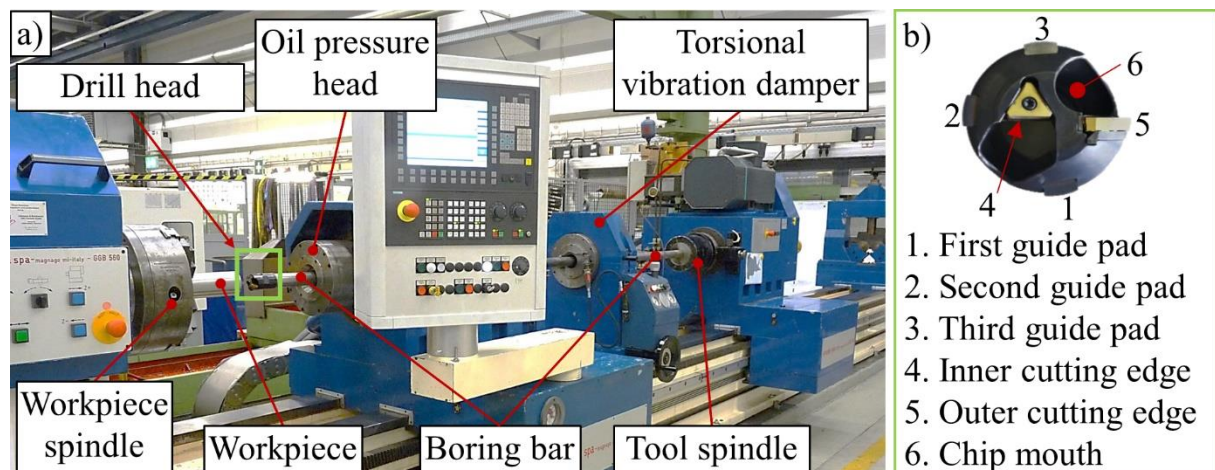

Fig. 1:   Setup employed for BTA deep hole drilling: a) Giana GBB 560, b) BTA drill head [10]

Sections in longitudinal and transverse directions were extracted from the middle of the bores at a length of $l = 120$ mm for light microscopy and microhardness analysis (Fig. 2 a). Microhardness mappings were performed by means of the hardness tester Shimadzu HMV-G21 in the longitudinal sections. Ten lines of six HV 0.01 impressions were set for each specimen according to the scheme displayed in Fig. 2 by applying a force of $F = 0.098$ N for a time of $t = 10$ s.
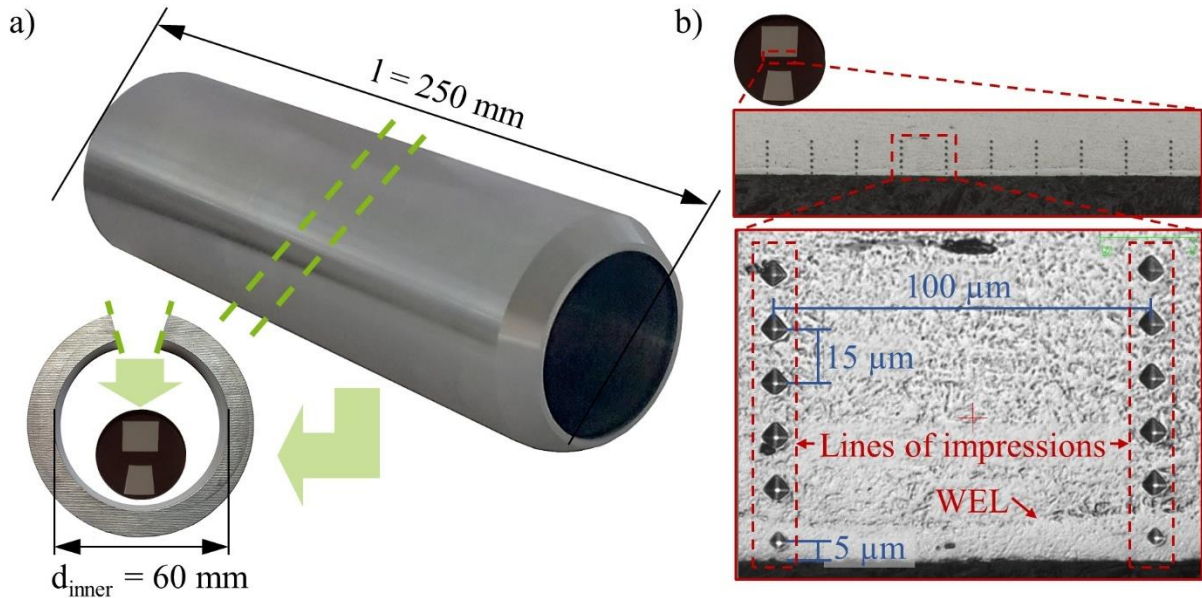
Fig. 2: Preparation of the specimens: a) extraction of segments from the deep drilled specimens, b) procedure for microhardness mappings, the specimen shown is machined by TiN-coated elements, a cutting speed of $v_c = 120$ m/min and a feed of $f = 0.225$ mm

The distance between impressions as well as between the first impressions and the embedding resin exceeds the standard for microhardness measurements according to Vickers as defined in DIN EN ISO 6507-1. However, positioning the impressions in this way allows for assessing the microhardness right in the WEL and for this reason it is a well-established practice [7,11,12].

MBN-based evaluation of SI at the middle of the bores was carried out before extracting segments. In MBN analyses, a periodically changing external magnetic field is applied to a ferromagnetic material. The magnetic field causes rapid jumps of the Bloch walls inside the material, which divide the magnetic domains. The intensity of these jumps is influenced by e.g. residual stresses, hardness and microstructural aspects like grain size [9]. Thus this versatile technique can be used for non-destructively analyzing all of these aspects of surface integrity in a very efficient, timesaving manner. Based on this, the application of MBN for the detection of WEL seems highly promising, since WEL are well known to have high hardness, elevated residual stresses and ultrafine grains.

All MBN analyses were performed using the device FracDim by Fraunhofer IKTS. A multipurpose sensor was placed in a custom-made positioning device, which allowed for locating the sensor accurately inside the bores. The system, the sensor and the positioning device used are depicted in Figure 3. All analyses were performed using a magnetization frequency of $f_{mag} = 60$ Hz, a magnetic field strength of $\phi_{mag} = 4.7$ µVs and a bandpass filter of $f_{min} = 10$ kHz to $f_{max} = 200$ kHz.
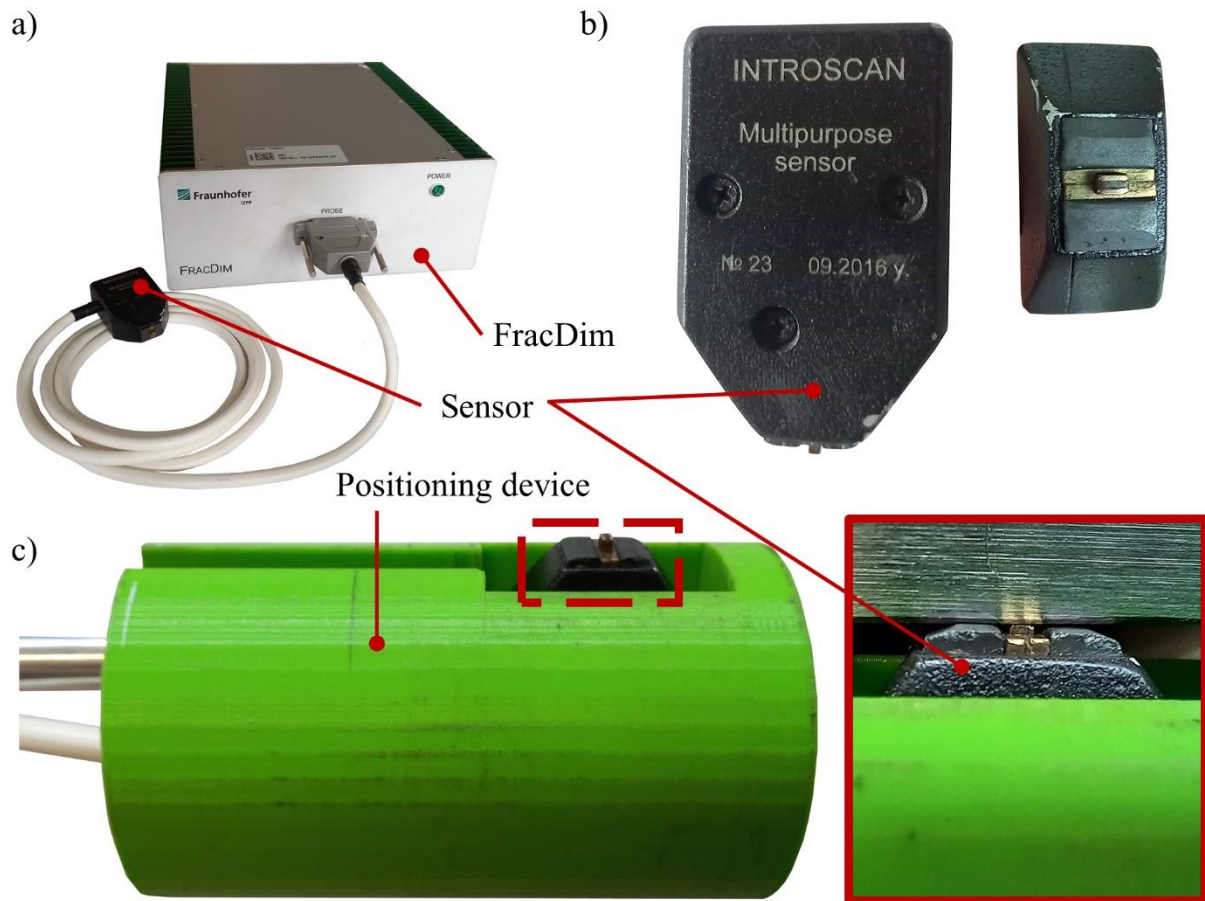
Fig. 3:   Equipment used for micromagnetic analyses: a) FracDim system by Fraunhofer IKTS, b) multipurpose sensor, c) multipurpose sensor mounted inside the custom-made positioning device for measurements inside of the bores

3   Results and discussion

In the following subchapters, the results of investigations will be presented and discussed. Micrographs of longitudinal and transverse sections of the bores will be shown (3.1). In addition to this, the results of microhardness mappings of the longitudinal sections will be presented (3.2) and the results of non-destructive, micromagnetic analyses of the subsurface of the bores will be given (3.3).

3.1 Results of the metallographic analyses

Figure 4 displays the micrographs obtained analyzing the longitudinal (Fig. 4a) and transverse (Fig. 4b) sections extracted from the bores machined with uncoated cutting edges and guide pads. It can be observed that thick WEL formed in drilling particularly at relatively high feeds (f ≥ 0.225 mm) and cutting speeds (v_c ≥ 80 m/min). Specimens drilled with lower feeds and cutting speeds show either no WEL at all or relatively thin and fragmented WEL. The thickest WEL using uncoated guide pads and cutting inserts

occurred at a cutting speed of $v_c = 80$ m/min and a feed of $f = 0.300$ and its thickness was approximately $t_{WEL} \approx 20$ µm.

Comparing sections in transverse and longitudinal directions, different shapes of WEL profiles are found. It can be observed that the sections measured in transverse direction showed relatively constant WEL thicknesses. In contrast to this, segments extracted in longitudinal direction exhibit a periodically increasing and decreasing WEL intensity. The distance between the maximum thicknesses in this periodic WEL profile corresponded to the employed feed. This observation indicates that the reason for the periodic profile of the WEL in longitudinal direction can be found in the contact conditions between the workpiece and cutting edge in between consecutive passes of the cutting edge.

Figure 5 depicts the micrographs of longitudinal (Fig. 5a) and transverse (Fig. 5b) sections extracted from the bores machined with TiN-coated guide pads and cutting edges. In all sections, apart from one (lowest feed and cutting speed, transverse section), WEL can be observed. As in the specimens machined with uncoated guide pads and cutting edges, higher feed rates and higher cutting speeds promote the formation of WEL. Again, the micrographs of feed direction (longitudinal) show a periodic profile, whereas in the cutting direction (transverse) there is a constant WEL thickness.

WEL thicknesses in the specimens machined with TiN-coated guide pads and cutting edges (Fig. 5) significantly exceed the WEL thicknesses in specimens machined with uncoated elements (Fig. 4). Based on this observation, the conclusion can be drawn that the coating of the cutting edges and guide pads promotes the formation of WEL. A reason for this can be the thermal conductivity of the TiN-coating, which is significantly lower than the thermal conductivity of cemented carbide. Thus, during drilling, more heat is passed on to the workpiece, since less heat is transferred into the tool, due to its coating, which acts as a thermal barrier. In previous investigations, it was shown that WEL can form in BTA deep hole drilling during machining by the cutting edges before the guide pads pass the surface [12]. Thus, the coating of the cutting edges might be a more decisive factor with respect to the formation of WEL compared to the coating of the guide pads.

When comparing the thickness of the WEL in the specimens machined with TiN-coated guide pads and cutting edges to the thickness of layers found in previous investigations, using a similar setup [7], it can be observed that the layers formed in this study are much thicker. An explanation for this can be found in dynamic process disturbances. During all drilling experiments, highly dynamic vibrations were observed. This might have led to higher temperatures and forces during drilling and subsequently the formation of thicker WEL, compared to a process with less dynamic disturbances.
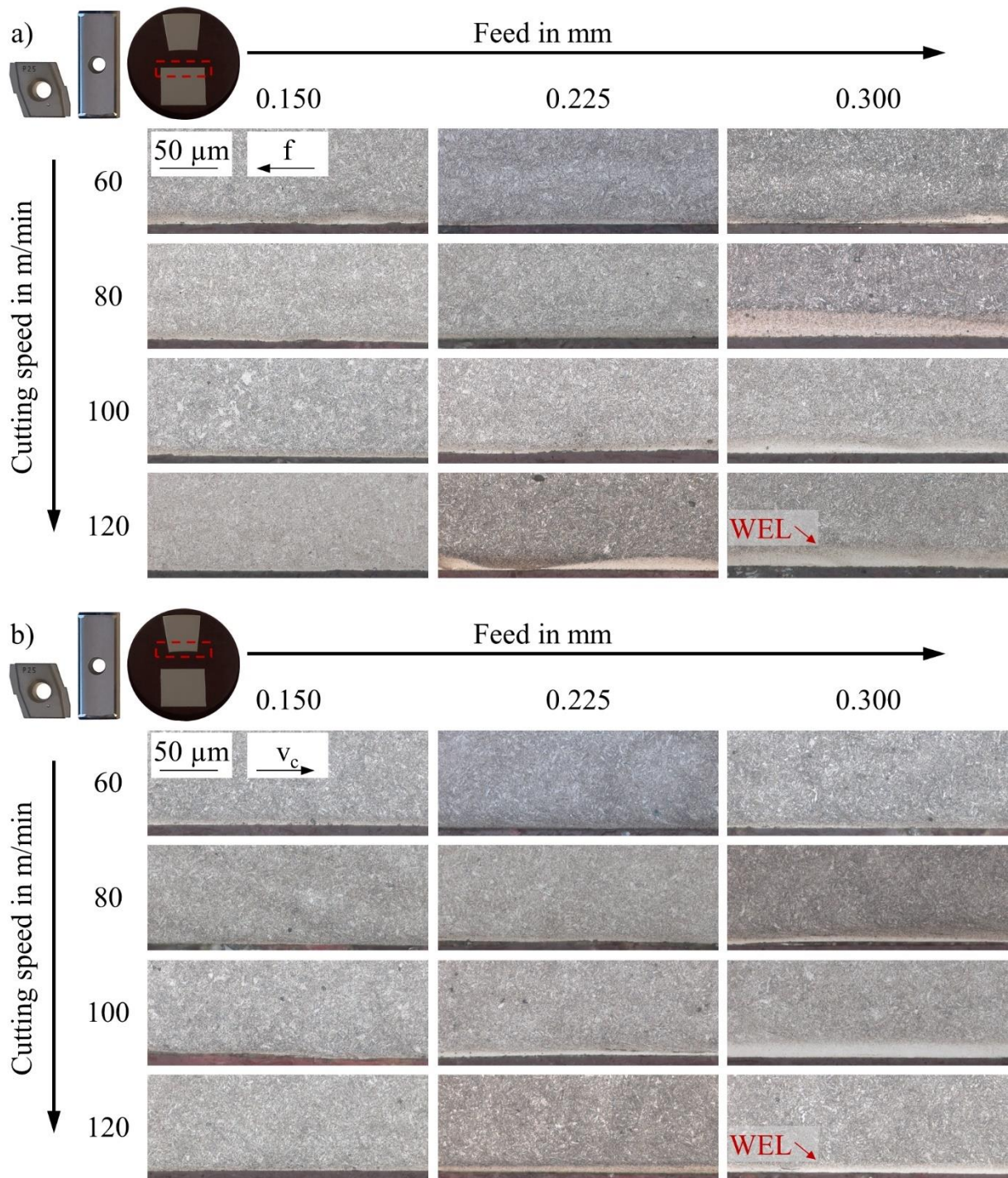
Fig. 4: Micrographs of the surfaces of the bores machined with uncoated cutting edges and guide pads: a) longitudinal sections, b) transverse sections
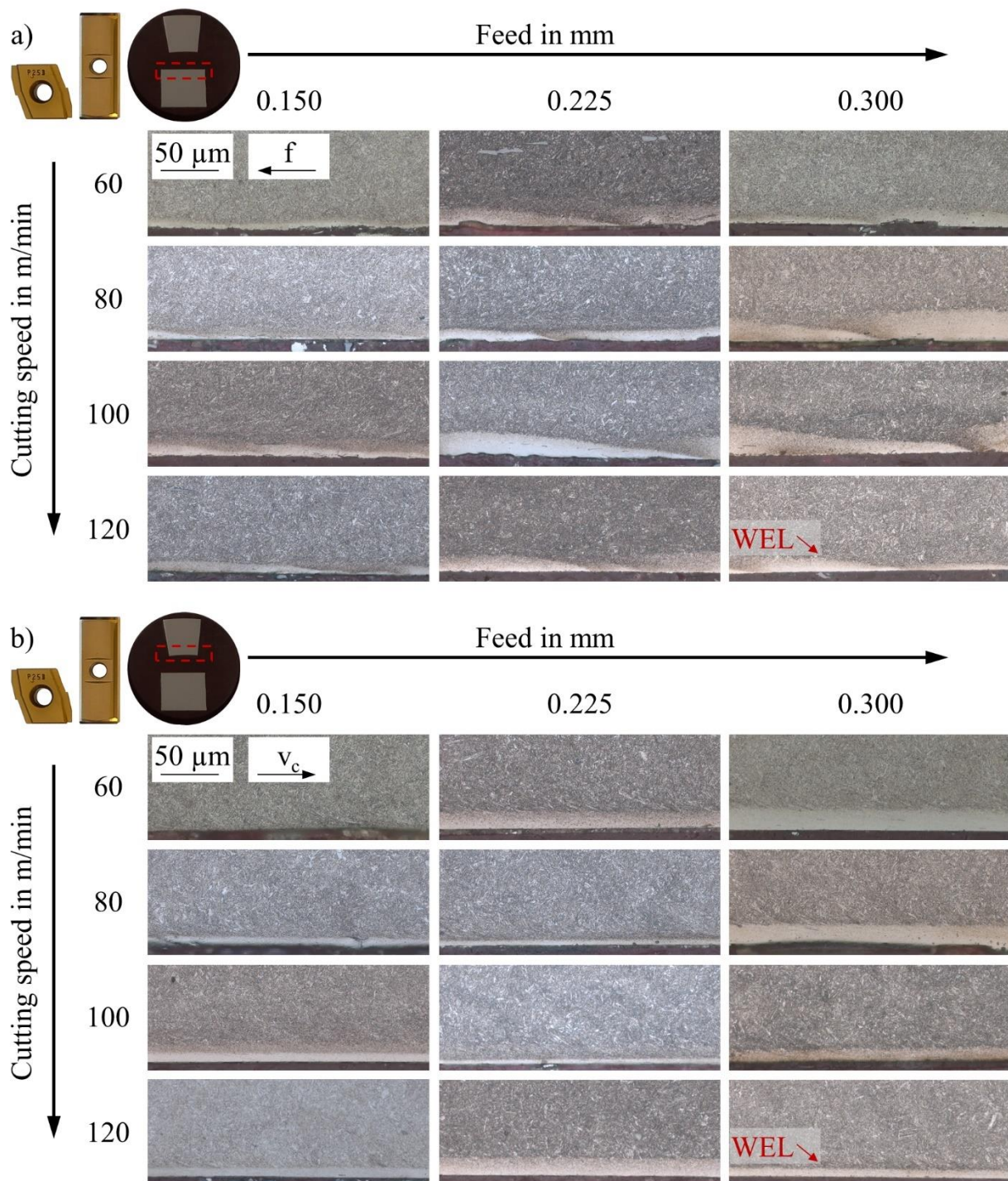
Fig. 5: *Micrographs of the surfaces of the bores machined with TiN-coated cutting edges and guide pads: a) longitudinal sections, b) transverse sections*

3.2 Results of the microhardness mappings

The results of microhardness mappings are displayed in Fig. 6 and Fig. 7. Figure 6 is a graphical illustration of the results of microhardness mappings for specimens drilled using uncoated (Fig. 6a) as well as TiN-coated (Fig. 6b) cutting edges and guide pads. The distances between the impressions displayed are depicted in Fig. 2. Figure 7 displays the results of microhardness mappings for the first three rows of impressions

(d_{surf} = 5; 20; 35 µm). The bars indicate the average hardness in each of the rows along with the standard deviation. It can be observed that for all specimens an increase in hardness close to the surface of the bore in the first row of impressions at a distance of d_{surf} = 5 µm occurs. Some of the specimens machined with TiN-coated cutting edges and guide pads show a significant increase in hardness also in the second row of impressions at a distance of d_{surf} = 20 µm.
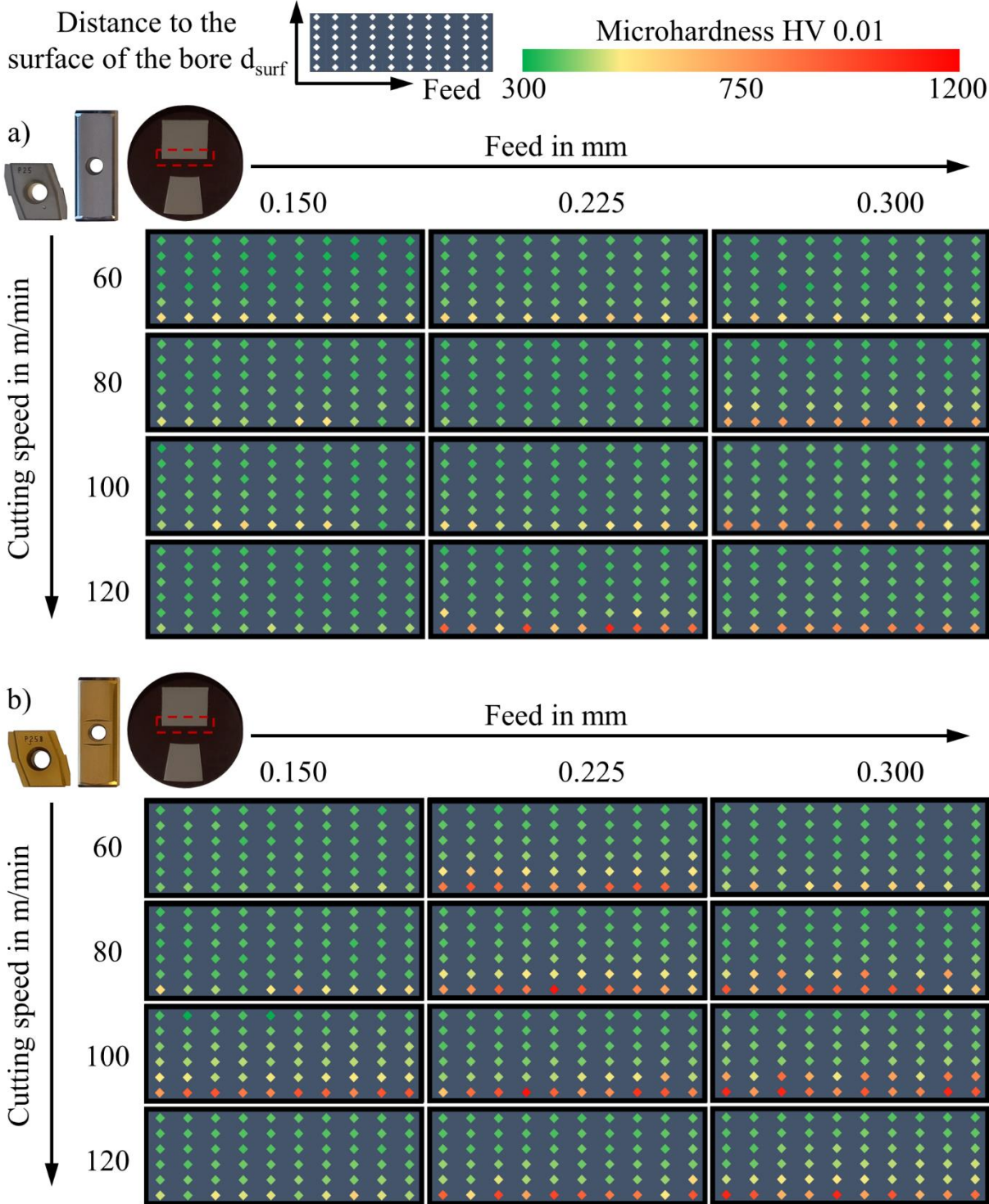

Fig. 6: *Microhardness mappings of the bores machined with a) uncoated cutting edges and guide pads and b) TiN-coated cutting edges and guide pads*
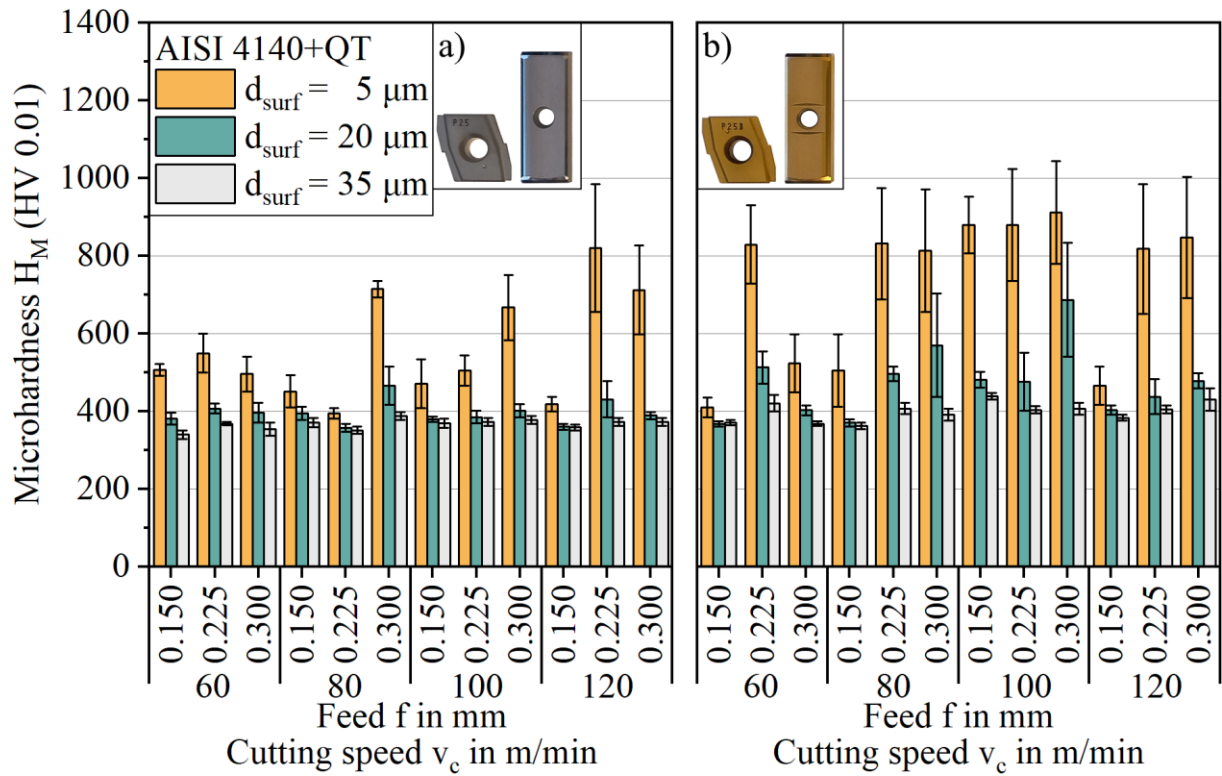
Fig. 7: *Microhardness close to the surface of the bores machined with a) uncoated cutting edges and guide pads and b) TiN-coated cutting edges and guide pads*

In the third row at a distance of $d_{surf} = 35$ µm, no significant difference can be observed and hardness is close to the hardness of the bulk material. The increase in hardness corresponds well with the results of metallographic analyses. Specimens that show thick WEL in their micrographs (Fig. 4, Fig. 5) have a significantly higher hardness close to the surface compared to specimens that are free from WEL (Fig. 6, Fig. 7). The hardness of the WEL exceeds the hardness of the bulk material by up to three times. Using TiN-coated cutting edges and guide pads leads to significantly higher hardness in the first two rows of impressions for most of the parameter combinations investigated. This can be attributed to the thicker WEL when using TiN-coated elements (Fig. 5). The relatively high standard deviation present for specimens with elevated hardness can be explained by the shape of WEL. Since microhardness mappings were performed analyzing the specimens extracted in longitudinal direction, the periodic shape of the WEL in this direction resulted in the impressions sometimes being inside of the WEL and sometimes right behind it and subsequently a high deviation between the calculated hardness. This periodicity can e.g. be observed in the microhardness mapping of the specimen machined with a cutting speed of $v_c = 100$ m/min and a feed of $f = 0.300$ mm and TiN-coated cutting inserts and guide pads (Fig. 6b).

2.3 Results of the micromagnetic analyses

The results of the micromagnetic MBN assessment are shown in Fig. 8. Analyzing the results for the bores machined with uncoated cutting edges (Fig. 8a), the lowest maximum MBN amplitudes M_{max} were found for the specimens drilled using relatively high feeds and cutting speeds. These specimens had thick WEL (Fig. 4a) and subsequently high hardness close to the surface of the bore (Fig. 6a). This corresponds well to the findings of previous investigations, that showed that the presence of WEL at a surface causes significantly lower MBN amplitudes [7]. The very high MBN amplitude for the specimen drilled with a cutting speed of $v_c = 60$ m/min and a feed of $f = 0.225$ might result from a distorted cutting process caused by damage to the outer cutting edge during drilling, which was observed after drilling.

In contrast to previous studies, specimens with relatively small and fragmented WEL (e.g. Fig. 4a, $v_c = 60$ m/min, $f = 0.150$ mm) could not be completely distinguished from specimens that seemed to be free of WEL (e.g. Fig. 4a, $v_c = 120$ m/min, $f = 0.150$ mm). A potential reason can be found in the inconsistent thickness of layers in combination with the size of the inspected area by the different methods and the micrographs shown might not be fully representative of the area assessed by MBN analyses.
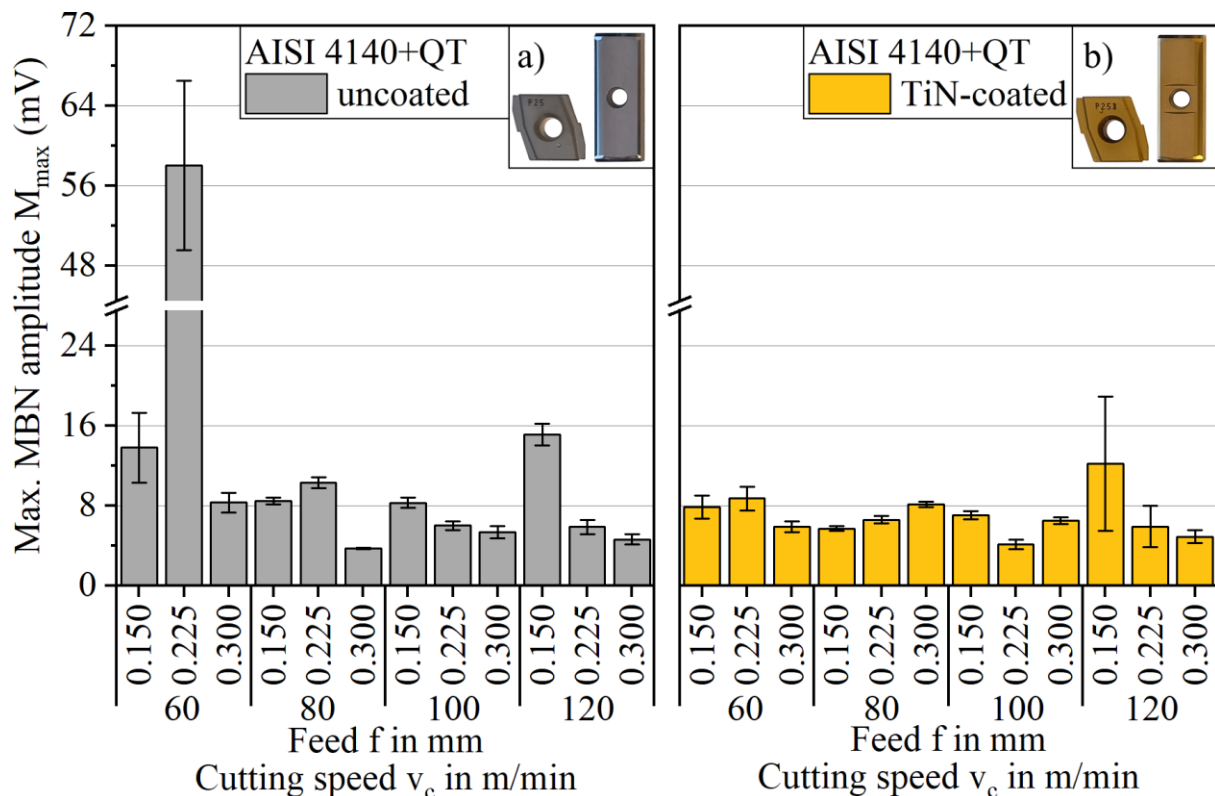

Fig. 8: Results of the micromagnetic analyses of the bores machined with a) uncoated cutting edges and guide pads and b) TiN-coated cutting edges and guide pads

Figure 8b depicts the findings of MBN analyses for bores machined with TiN-coated cutting edges and guide pads. Here, the discovered correlation is not fully applicable to all of the specimens. For some cutting speeds (e.g. v_c = 120 m/min) an increase in feed led to harder and thicker WEL and subsequently lower MBN amplitudes. However, for others (e.g. v_c = 80 m/min) this correlation does not fully apply. A possible explanation for this observation might be that other effects e.g. altered residual stresses might super-impose the effect of WEL on MBN amplitudes in these specimens. Since MBN is a holistic technique, it is sensitive to numerous characteristics of materials and high residual stresses might cover the effects of microstructure. In addition to this, time-dependent dynamic process disturbances can serve as an explanation for the deviations from the previously discovered correlations. During all drilling experiments, highly dynamic vibrations were observed, which might have led to an inconsistent SI in the specimens.

4   Conclusions and outlook

Depending on the design of the process, WEL form during BTA deep hole drilling. High feed rates and cutting speeds generally seem to promote the formation of WEL. Compared to uncoated cutting edges and guide pads, TiN-coated tools lead to WEL formation at lower cutting speeds and feeds as well as to significantly thicker WEL. An explanation for this can be found in the relatively low thermal conductivity of TiN and subsequently higher temperatures in the subsurface of the workpiece when using TiN-coated cutting edges and guide pads. This hypothesis will be tested in future investigations. In sections extracted in longitudinal direction, micrographs revealed a periodically increasing and decreasing thickness of the WEL. The periodicity of this shape corresponds to the feed employed in drilling. Sections extracted in transverse direction show relatively constant WEL thickness. In microhardness mappings, the hardness of WEL exceeds the hardness of the bulk material by up to three times. Looking at very thick WEL, significantly elevated hardness was still observed at a depth below the surface of the bore of d_{surf} = 20 µm. In micromagnetic investigations of the specimens machined with uncoated cutting edges and guide pads, the correlations discovered in previous investigations [7] are supported. Maximum MBN amplitudes are significantly lower in the specimens with thick WEL. This correlation does not fully apply to specimens machined with TiN-coated elements. Potential reasons for this might be found in the occurrence of dynamic disturbances during drilling. This will be checked with the aim of increasing the robustness of MBN analysis. Based on this, a closed-loop control will be developed for BTA deep hole drilling, to allow for the robust production of high-performance components that are free of WEL.

Acknowledgement

References

[1] Stampfer, B.; González, G.; Gerstenmeyer, M.; Schulze, V.: The present state of surface conditioning in cutting and grinding. Journal of Manufacturing and Materials Processing 5, 3 (2021) 1–17.

[2] Liao, Z.; La Monaca, A.; Murray, J.; Speidel, A.; Ushmaev, D.; Clare, A.; Axinte, D.; M'Saoubi, R.: Surface integrity in metal machining - Part I: Fundamentals of surface characteristics and formation mechanisms. International Journal of Machine Tools and Manufacture 162 (2021) 1–51.

[3] La Monaca, A.; Murray, J.; Liao, Z.; Speidel, A.; Robles-Linares, J.; Axinte, D.; Hardy, M.; Clare, A.: Surface integrity in metal machining - Part II: Functional performance. International Journal of Machine Tools and Manufacture 164 (2021) 1–55.

[4] Brown, M.; Wright, D.; M'Saoubi, R.; McGourlay, J.; Wallis, M.; Mantle, A.; Crawforth, P.; Ghadbeigi, H.: Destructive and non-destructive testing methods for characterization and detection of machining-induced white layer: A review paper. CIRP Journal of Manufacturing Science and Technology 23 (2018) 39–53.

[5] Brown, M.; Pieris, D.; Wright, D.; Crawforth, P.; M'Saoubi, R.; McGourlay, J.; Mantle, A.; Patel, R.; Smith, R.; Ghadbeigi, H.: Non-destructive detection of machining-induced white layers through grain size and crystallographic texture-sensitive methods. Materials & Design 200, 109472 (2021) 1–13.

[6] Biermann, D.; Bleicher, F.; Heisel, U.; Klocke, F.; Möhring, H.-C.; Shih, A.: Deep hole drilling. CIRP Annals 67, 2 (2018) 673–694.

[7] Strodick, S.; Berteld, K.; Schmidt, R.; Biermann, D.; Zabel, A.; Walther, F.: Influence of cutting parameters on the formation of white etching layers in BTA deep hole drilling. Technisches Messen 87, 11 (2020) 674–682.

[8] Zhang, H.; Shen, X.; Bo, A.; Li, Y.; Zhan, H.; Gu, Y.: A multiscale evaluation of the surface integrity in boring trepanning association deep hole drilling. International Journal of Machine Tools and Manufacture 123 (2017) 48–56.

[9] Baak, N.; Hajavifard, R.; Lücker, L.; Rozo Vasquez, J.; Strodick, S.; Teschke, M.; Walther, F.: Micromagnetic approaches for microstructure analysis and capability assessment. Materials Characterization 178, 111189 (2021) 1–14.

[10] Strodick, S.; Schmidt, R.; Brause, L.; Zabel, A.; Biermann, D.; Walther, F.: Micromagnetic characterization of the bore integrity (in German). wt Werkstattstechnik online, 11/12 (2022) 757–761.

[11] Nickel, J.; Baak, N.; Walther, F.; Biermann, D.: Influence of the feed rate in the single-lip deep hole drilling process on the surface integrity of steel components. Proceedings of the 1st International conference on Advanced Surface Enhancement (2020) 198–212.

[12] Strodick, S.; Schmidt, R.; Biermann, D.; Zabel, A.; Walther, F.: Influence of the cutting edge on the surface integrity in BTA deep hole drilling - part 2: Residual stress, microstructure and microhardness. Procedia CIRP 108 (2022) 276–281.

Author's address

Simon Strodick

TU Dortmund University

Chair of Materials Test Engineering (WPT)

Baroper Str. 303

D-44227 Dortmund

Phone: +49 231 755 90161

Fax: +49 231 755 8029

Email: simon.strodick@ tu-dortmund.de